Available online at www.sciencedirect.com
SCIENCE DIRECT®
Polymer 44 (2003) 7405–7412
polymer
www.elsevier.com/locate/polymer

In situ FTIR microscope study on crystallization of crystalline/crystalline polymer blends of bacterial copolyesters

Naoko Yoshie[a,*], Akeshi Asaka[b], Koji Yazawa[b], Yasufumi Kuroda[b], Yoshio Inoue[b]

[a]*Institute of Industrial Science, The University of Tokyo, Komaba 4-6-1, Meguro-ku, Tokyo 153-8505, Japan*
[b]*Department of Biomolecular Engineering, Tokyo Institute of Technology, 4259 Nagatsuta, Midori-ku, Yokohama 226-8501, Japan*

Received 17 July 2003; received in revised form 4 September 2003; accepted 17 September 2003

Abstract

This study describes in situ observation of crystallization in a spherulite of blends of poly(3-hydroxybutyrate-*co*-3-hydroxyvalerate) [PHBV] and poly(3-hydroxybutyrate-*co*-3-hydroxypropionate) [PHBP] by FTIR microscopy. In order to trace the crystallization processes of blend components separately, PHBV was deuterated. The C–D and C=O stretching bands in the IR spectra, respectively, show the crystallization behavior of PHBV and the whole blend. D-PHBV containing 6 and 8% HV [D-PHBV6 and D-PHBV8] are blended with PHBP containing 11% HP [PHBP11]. The crystallization rates of D-PHBV6, D-PHBV8 and PHBP11 decrease in this order. In case of the blend of D-PHBV8 and PHBP11 the crystalline peaks of C–D and C=O bands grows simultaneously during crystallization, and the growth rates are rather close to that of D-PHBV8. The results indicate that D-PHBV8, which is the component that shows higher crystallization rate in the pure state, leads the cocrystallization of the blend. For D-PHBV6/PHBP11, on the other hand, the crystalline peak of C–D band grows faster than that of C=O band, indicating that the crystallization of D-PHBV6 proceeds before the crystallization of PHBP11. During the crystallization of D-PHBV6, PHBP11 molecules get away from the growing front of the spherulite, i.e. the phase segregation precedes the crystallization. These results demonstrate that FTIR microscopy is a powerful tool to trace the formation of different crystalline phases, such as cocrystallization and phase segregation.

Keywords: Crystalline/crystalline polymer blend; IR microscopy; In situ observation of crystallization

1. Introduction

Many studies on the phase structure and the morphology of miscible crystalline/amorphous polymer blends have been reported. In such blends, the amorphous component escapes from the growing front of crystals and resides in interspherulitic, interfibrillar, and/or interlamellar regions. The extent of the phase segregation depends on the crystallization rate of the crystalline component, the chain mobility of the amorphous component and the strength of the intermolecular interactions between the components. Faster crystallization of the crystalline component, lower mobility of the amorphous component, and stronger attractive force between the components make the amorphous component stay closer to the crystalline lamellas. These factors also influence to the microstructure of the crystalline component, such as degree of crystallinity and lamellar thickness. On the other hand, the mechanism of the phase formation in crystalline/crystalline polymer blends is less well understood. The ability of the second component to crystallize broadens the variation of the possible phase structures [1–10]. The crystallization of one component suppresses the crystallization of the other in some cases and both components simultaneously crystallize in the other cases. In the latter cases, the components can exist inside a lamella, in separate lamellas inside a fibril, in separate fibrils inside a spherulite, or in separate spherulites. Among these structures, the cocrystallization in a lamella is a rare phenomenon observed only when the chemical structures of two component polymers are very similar. Various level of the phase separation also occurs in the amorphous phase. Though the complicated structure of crystalline/crystalline polymer blends makes the systematic analysis difficult, it attracts of considerable technological interest and offers the challenging research area.

Poly(3-hydroxybutyrate) [PHB] and its copolymers with

* Corresponding author. Tel.: +81-354526309; fax: +81-354526311.
E-mail address: yoshie@iis.u-tokyo.ac.jp (N. Yoshie).

0032-3861/$ - see front matter © 2003 Elsevier Ltd. All rights reserved.
doi:10.1016/j.polymer.2003.09.024

other 3-hydroxyalkanoate have been extensively studied as a biodegradable and biocompatible thermoplastic [11]. Studies on the blends of PHB with its copolymers such as poly(3-hydroxybutyrate-*co*-3-hydroxyvalerate) [PHBV] [12–14] and poly(3-hydroxybutyrate-*co*-3-hydroxypropionate) [PHBP] [15] are among them. PHBV keeps high crystallinity throughout a range of composition from 0 to 100% HV due to the isomorphous behavior [16,17]. PHBP is also semicrystalline when the HP content is less than 30 mol% and more than 70 mol%. So, PHB/PHBV and selected PHB/PHBP blends are crystalline/crystalline polymer blends. These blends provide a wide variety of phase structures from cocrystallization to immiscible phase separation, which can be controlled by careful selection of the HV or HP content, f_{co}, of PHBV or PHBP and sample preparation conditions. The copolymers cocrystallize with PHB in lamellas when f_{co} is less than 10 mol%. When f_{co} exceeds this level, the copolymer content in lamellas decreases, and finally, the copolymer forms separate crystallites even in the miscible blend. When f_{co} exceeds 30–40 mol%, the blends become immiscible. Though the microstructures of these blends were elucidated as just described, there are few reports on the crystallization dynamics. Since crystallization and phase segregation of these blends are controlled by kinetic factors, observation of the dynamic process is fundamental for the complete understanding of their structures.

In this study, we report on in situ observation of the crystallization of the blends of PHBV and PHBP by FTIR microscopy. This pair of copolymers is selected for two reasons. (1) Since both PHBV and PHBP are crystallized in the same PHB-type crystalline lattice, we expected to occur the cocrystallization of the two component polymers. (2) The spherulite growth rates of PHBV and PHBP with HV or HP content of 0–20 mol% are suitable for the real-time observation by FTIR microscope. In order to trace the crystallization process of the blend components separately, deuterated PHBV (D-PHBV) is blended with normal PHBP. The C–D and C=O stretching bands of the IR spectra are used to trace the crystallization of D-PHBV and the whole blend, respectively. The spherulites of D-PHBV and PHBP grow to a few hundreds micrometers in diameter at a certain crystallization temperature range. FTIR microscope allows the observation inside a spherulite by setting an aperture area of a few dozen micrometers in size.

2. Experimental section

2.1. Materials

D-PHBV and PHBP samples were prepared by fermentation of *Ralstonia eutropha* H16 (ATCC17699) and *Alcaligenes latus* (ATCC 29713), respectively, as previously reported [18,19]. Carbon sources used for the biosynthesis of D-PHBV and PHBP are a mixture of acetic acid-d_4 and propionic acid-d_5 and a mixture of (R)-3-hydroxybutyric acid and 3-hydroxypropionic acids, respectively. After extraction from the dried cells with hot chloroform, the copolyesters were compositionally fractionated by using chloroform/heptane mixed solvent [20,21].

D-PHBV containing 6 and 8 mol% HV [D-PHBV6 and D-PHBV8] and PHBP containing 11% HP [PHBP11] were used in this study. Molecular characteristics of these copolymers are listed in Table 1. Molecular weight characterization was performed by gel-permeation chromatography (GPC) equipped with a refractive detector. Polystyrene standards with a low polydispersity were used to construct a calibration curve. ^{2}H content and comonomer composition was determined by ^{1}H and ^{2}H NMR spectroscopy. It has been known that even if per-deuterated carbon source is used for the biosynthesis, only partially deuterated polyesters are produced due to the substitution of ^{2}H with ^{1}H during the metabolic process of the polyester synthesis [22,23]. The ^{2}H contents in main-chain methine, main-chain methylene, and side-chain groups of D-PHBV were 0.25, 0.65, and 0.75, respectively, which gave the average ^{2}H content as 0.65. The amount of ^{2}H of D-PHBV is enough for the observation of the C–D bands by FTIR microscope. For D-PHBV, the HV contents determined by ^{1}H and ^{2}H NMR spectra agree within a range of experimental error indicating that the ^{2}H contents of HV and HB units are similar. Only the data determined from ^{1}H NMR spectra are shown in Table 1. Spherulite growth rate of the samples was measured by a polarized microscope equipped with a hot stage. Samples were heated to 195 °C, kept at this temperature for 1 min and then cooled to a selected crystallization temperature (90 °C) where they were kept isothermally. The spherulite growth rate was taken as the slope of the linear plot of spherulite radius versus time.

Blending of samples was performed by a conventional solvent-casting technique from chloroform solution using a glass Petri dish as a cast surface. 0/1, 1/3, 1/1, 3/1, and 1/0 (w/w) blends of D-PHBV6/PHBP11 and D-PHBV8/PHBP11 were prepared.

2.2. FTIR Microscopy

Time-resolved FTIR measurements during isothermal crystallization of samples were carried out by using a SHIMADZU AIM-8800 FTIR microscope equipped with a Mettler FP82HT hot stage. A cast film was heated to 195 °C, kept at this temperature for 1 min and then cooled to 90 °C where it was kept isothermally. A growing spherulite residing apart from the others was found visually under polarized light. A square aperture of 30 × 30 μm was set parallelized to and apart from the growing front of it. Fig. 1 shows the visual images of a growing spherulite of PHB observed by the FTIR microscope apparatus. The square in the images represents the aperture. Time was set to be zero just when the growing front of a spherulite enters the

Table 1
Molecular characteristics of PHBP and D-PHBV

Polyester	HV content/mol%[a]	$M_w \times 10^{-5}$[b]	M_w/M_n[b]	Spherulite growth rate/μm s^{-1}[c]
D-PHBV6	5.9	14.6	1.8	2.31
D-PHBV8	8.0	14.8	1.8	1.44
PHBP11	11.1	3.2	1.8	0.25

[a] Measured by ^{1}H NMR.
[b] Measured by GPC.
[c] Growth rate at 90 °C determined with a polarized microscope equipped with a hot stage.

aperture area (Fig. 1(a)). The time just when the growing front exits from this area was defined as t_{pass} (Fig. 1(b)). A series of FTIR spectra were recorded with a resolution of 4 cm^{-1} at specified time intervals. The measurements were started well before the growing front of the spherulite went into the aperture and continued long after the front left the aperture. The crystallization of samples was traced by the C=O stretching band at 1722 cm^{-1} and the C–D stretching band at 2230 cm^{-1}. Because of the large difference in the molar absorbance coefficients, the C=O and C–D stretching bands were observed by separate measurements. A thick film sample on a BaF_2 plate was used for the C–D band observation, while a thin sample inserted between the BaF_2 plates was used for the observation of the C=O band.

2.3. Thermal analysis

Melting behavior of isothermally crystallized samples was analyzed. Cast-film samples were inserted between aluminum plates with an aluminum spacer (0.1 mm thickness) and were compression-molded at 195 °C for 3 min under a pressure of 5 MPa by using a Toyoseiki Mini Test Press-10. The molten samples were then cooled to 90 °C and kept for four weeks to reach the equilibrium crystallinity. Thermal analysis was carried out by a SEIKO EXSTAR6000 system equipped with a DSC 220U. The isothermally crystallized samples of 2–3 mg in aluminum pans were heated from 30 to 200 °C at a heating rate of 10 °C/min. The melting temperature was taken as the position of the melting peak.

3. Results and discussion

3.1. Thermal analysis of D-PHBV/PHBP

Fig. 2 shows the DSC melting curves of D-PHBV8/PHBP11 and D-PHBV6/PHBP11 blends and their component copolymers crystallized at 90 °C. All the samples excepting pure D-PHBV8 and PHBP11 show two-peak melting behavior. Two melting peaks are often observed on the melting curve of semicrystalline polymers and polymer blends. When the two-peak behavior is interpreted, it is important to distinguish multiple peaks arising from phase-separated structures and those arising as a result of a melt/recrystallization process. We differentiated between them by simply varying the heating rate [24]. For all the samples showing two-peak melting, the relative intensity of the higher temperature peak decreased with the increase of the heating rate (data not shown). Therefore, the higher melting peak is ascribed to the melt/recrystallization process during heating in DSC apparatus while the lower temperature peak corresponds to the melting of crystals formed at the crystallization temperature (90 °C). In other words, all the samples of D-PHBV8/PHBP11 and D-PHBV6/PHBP11 form only one crystalline phase, indicating the miscibility of these blends. This result was supported by the observation of the melt state by polarized optical microscopy. No sign of phase separation was observed (data not shown).

Fig. 3 shows the variation in the melting temperature with weight fraction of PHBP11 for D-PHBV8/PHBP11 and D-PHBV6/PHBP11 blends crystallized at 90 °C, respectively. The melting temperature of D-PHBV8/PHBP11 blends lies on a straight line connecting the melting

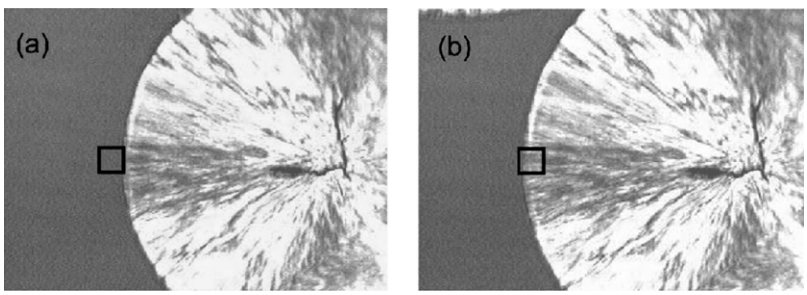

Fig. 1. Crossed polar images of a growing spherulite of PHB observed by the FTIR microscope at $t = 0$ (a) and $t = t_{pass}$ (b). The square in the image represents the aperture of 30 × 30 μm.

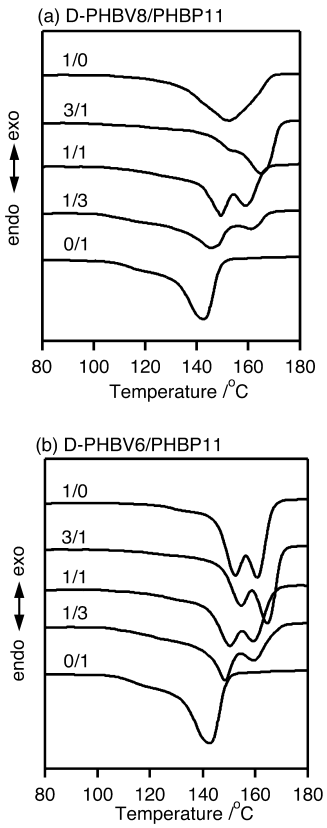

Fig. 2. DSC melting curves for 1/0, 3/1, 1/1, 1/3 and 0/1 blends of (a) D-PHBV8/PHBP11 and (b) D-PHBV6/PHBP11 crystallized at 90 °C.

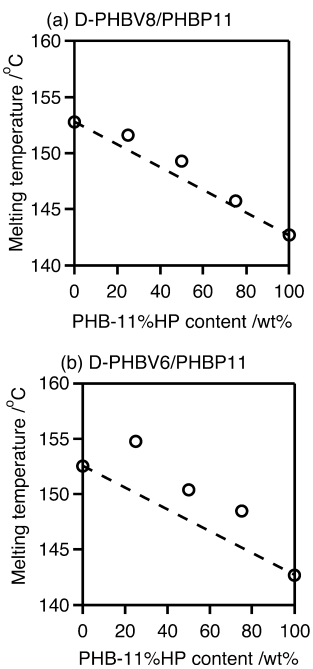

Fig. 3. Variation in the melting temperature with weight fraction of PHBP11 for (a) D-PHBV8/PHBP11 and (b) D-PHBV6/PHBP11 crystallized at 90 °C.

temperatures of the component polymers, D-PHBV8 and PHBP11. The linear relationship between melting temperature and blend composition indicates that PHBP11 cocrystallize with D-PHBV8 [14]. The PHBP11 content in the crystalline region is similar to the blend composition. On the other hand, the plot of melting temperature for D-PHBV6/PHBP11 blends becomes convex upward, indicating the phase segregation [14]. PHBP11 molecules escaped from the growing front of the crystals, and as a result, the crystalline phase of these blends are suggested to be mainly composed of D-PHBV6. Note that the melting temperature of 3/1 D-PHBV6/PHBP11 is rather higher than those of pure D-PHBV6 and pure PHBP11, although melting temperatures lower than those of the component polymers is rather expected for usual polymer blends. This result suggests that the lamellas in the blend are thicker than those of pure D-PHBV6. As shown later, the existence of PHBP11 makes the crystallization slower, which may lead thicker lamellas.

3.2. FTIR microscopy of D-PHBV

Before describing the FTIR microscope analysis of D-PHBV/PHBP blends, the changes of the C=O and C–D stretching bands during the crystallization of pure D-PHBV and PHBP are described. Fig. 4 shows the time resolved C=O and C–D stretching bands of D-PHBV8 during

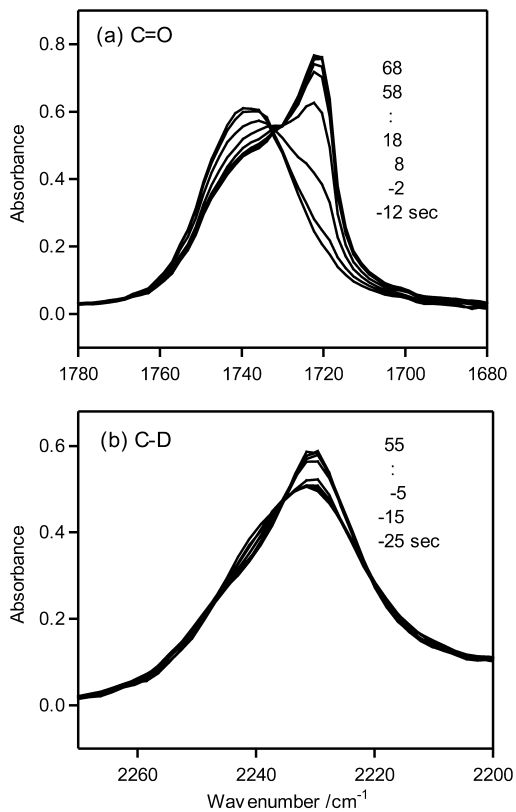

Fig. 4. Time resolved C=O (a) and C–D (b) stretching bands of D-PHBV8 measured during isothermal crystallization at 90 °C observed by FTIR microscope.

isothermal crystallization at 90 °C. The C=O and C–D bands are approximately symmetrical before the growing front of the spherulite enters into the aperture area ($t < 0$) while additional peaks begin to appear at lower wavenumber side of these bands when the growing front enters this area ($t > 0$). These peaks must be ascribed to the crystalline phase.

In a previous paper [25], the C=O band of PHB was curve-resolved into three symmetrical (one Lorenzian and two Gaussian) peaks ascribed to the crystalline, amorphous and interfacial phases, respectively. Though this three-peak model is also an appropriate model of the C=O band for D-PHBV and PHBP, we adopt a simpler model in this study. The C=O and C–D bands are analyzed with the assumption that the bands are comprised of the two peaks from the crystalline and amorphous phases, respectively. It should be noted that these peaks are not constrained to be symmetrical in order to open the way for counting the contributions of the interfacial phase. Only the assumption imposed on this two-peak model is that the absorption coefficients of crystalline and amorphous phases at 1722 cm^{-1} (C=O band) and 2230 cm^{-1} (C–D band) are constant during the crystallization process. In this model, the absorbance $A(\nu, t)$ at wavenumber ν ($\nu = 1722$ or 2230 cm^{-1}) and time t is given by

$$A(\nu, t) = \{\chi(t)\varepsilon_{cry}(\nu) + [1 - \chi(t)]\varepsilon_{amos}(\nu)\}l \quad (1)$$

where l, $\chi(t)$, $\varepsilon_{cry}(\nu)$, and $\varepsilon_{amos}(\nu)$ are sample thickness, mole fraction of crystalline parts at time t, and absorption coefficients of crystalline and amorphous phases at ν, respectively.

Considering that the absorbance, $A(\nu, -\infty)$, well before the growing spherulite reaches the aperture area is equal to the absorbance of complete amorphous samples, the relative degree of crystallinity, $X(\nu, t)$, at time t is given by

$$X(\nu, t) = \chi(t)/\chi(\infty)$$
$$= [A(\nu, t) - A(\nu, -\infty)]/[A(\nu, \infty) - A(\nu, -\infty)] \quad (2)$$

where $t = \infty$ indicates the time when PHB has reached equilibrium crystallinity. $A(\nu, \infty)$ is given by the spectrum measured well after the growing front of the spherulite leaves the aperture area.

Fig. 5 shows the time dependence of the relative crystallinity, $X(\nu, t)$, for PHBP11 and D-PHBV8 crystallized at 90 °C. At this temperature, t_{pass} for PHBP11, and D-PHBV8 are 120 and 21 s, respectively.

Since the aperture is set far from the center of the spherulite in this analysis, the aperture area occupied by the spherulite increases at a constant rate from $t = 0$ to $t = t_{pass}$. Supposing that the crystallization is completed instantaneously at the exact position of the growing front, the relative crystallinity, $X(\nu, t)$, is expected to increase linearly with time. Contrary to this, however, the time dependence of $X(\nu, t)$ for PHBP and D-PHBV shows sigmoid curves (see also $X(1722, t)$ for D-PHBV6 shown in Fig. 6(b)). Furthermore, $X(\nu, t)$ begins to increase before the growing front of the spherulite enters the aperture area ($t < 0$) and as

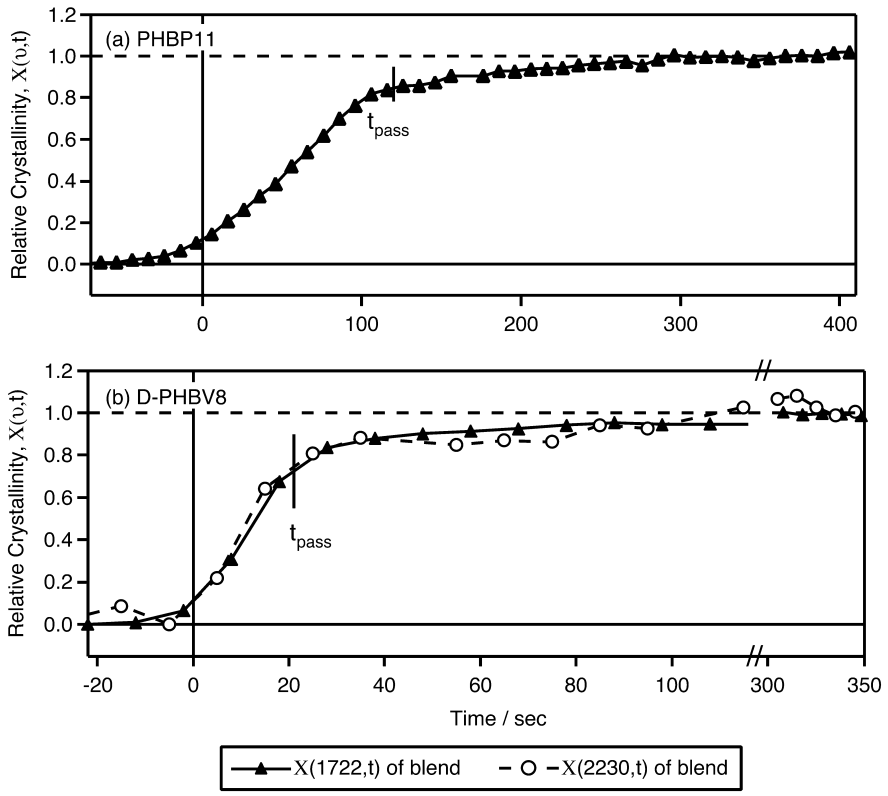

Fig. 5. Time dependence of the relative crystallinity $X(1722, t)$ and $X(2230, t)$ for (a) PHBP11 and (b) D-PHBV8 crystallized at 90 °C.

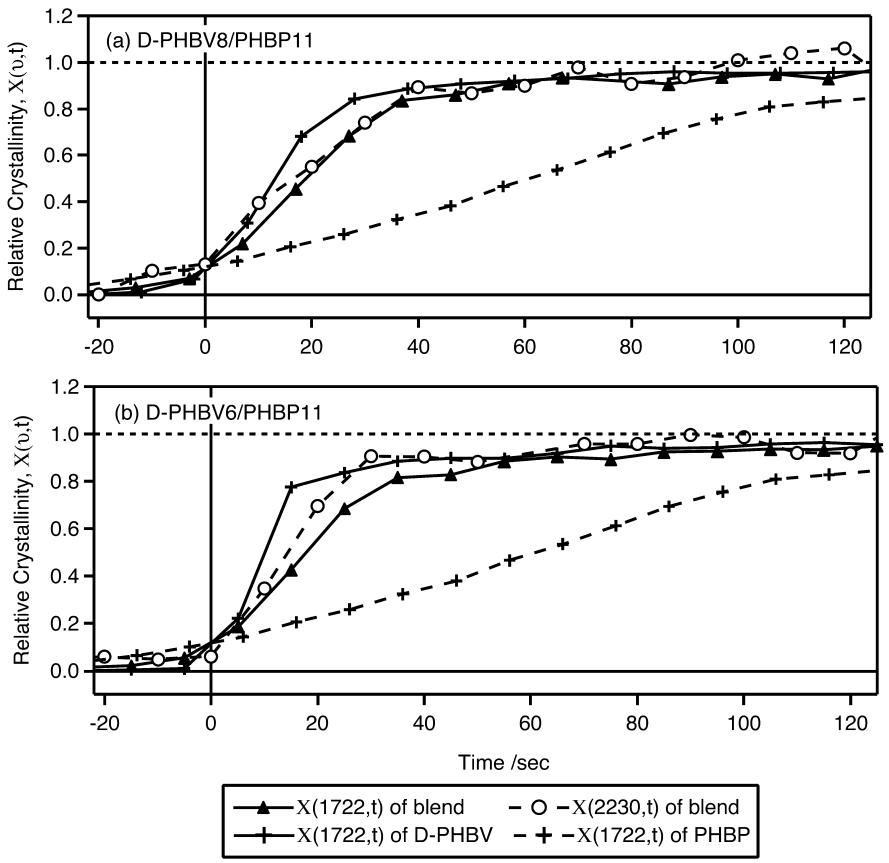

Fig. 6. Time dependences of $X(1722, t)$ and $X(2230, t)$ of 1/0, 1/1 and 0/1 blends of (a) D-PHBV8/PHBP11 and (b) 1/1 D-PHBV6/PHBP11.

a result, $X(\nu, 0) \approx 0.1$ at $t = 0$. This fact may be partially ascribed to some kind of conformational change that happens before the formation of spherulite becomes visible. However, the main cause of it must be diffraction of IR light. After light has passed through the aperture, it spreads out to a certain extent, reaches the sample area where the aperture is expected to mask, and as a result, skews the spectrum depending on the state of the sample in this area. Hence, when the growing front of the spherulite reaches just outside the aperture, part of diffracted light passes through the spherulite and gives the spectrum of the crystalline state. Though light diffraction also contributes to the increase of $X(\nu, t)$ at $t > t_{pass}$, the pattern of $X(\nu, t)$ at $t > t_{pass}$ is apparently different from that at $t < 0$. $[1 - X(\nu, t_{pass})]$ is slightly larger than $X(\nu, 0)$ and $X(\nu, t)$ at $t > t_{pass}$ grows over longer period than that at $t < 0$. This result suggests that the secondary crystallization contribute the growth of $X(\nu, t)$ at $t > t_{pass}$.

Fig. 5(b) demonstrates that the time dependence of $X(2230, t)$ completely accords with that of $X(1722, t)$ for D-PHBV8. It has been reported that for the case of polystyrene [26,27] and poly(bisphenol A-*co*-decane ether) [28], the absorbances of IR bands change not simultaneously but rather sequentially during the crystallization. These sequential changes were interpreted as the hierarchical conformational change. Though this kind of behavior is advantageous for, for example, the detection of the transient liquid phase preceding the crystallization, it is undesirable for the present study which aims to evaluate the time cause of the crystallization of respective blend components through the comparison of the bands ascribed to one component and to the whole blend. A pair of bands that reflect the same conformational change or synchronizing conformational changes is required. Fortunately, the time dependence of $X(2230, t)$ completely agrees with that of $X(1722, t)$ for D-PHBV8 as shown in the figure, indicating these parameters reflect the synchronized conformational changes during crystallization. The same result was obtained for D-PHBV6. The time dependence of $X(2230, t)$ (data not shown) completely agreed with that of $X(1722, t)$ (shown in Fig. 6(b)) for D-PHBV6. Therefore, we can evaluate the crystallization processes of the components in D-PHBV/PHBP blends separately through the comparison of $X(1722, t)$ and $X(2230, t)$.

3.3. FTIR microscopy of D-PHBV/PHBP blends

Fig. 6 show the time dependences of $X(1722, t)$ and $X(2230, t)$ of 1/1 D-PHBV8/PHBP11 blend and 1/1 D-PHBV6/PHBP11 blend crystallized at 90 °C. $X(1722, t)$ of the component copolymers are also plotted. For the blends, $X(1722, t)$ reflects the crystallization behavior of the overall

blends, while $X(2230, t)$ allows to pick out the information on D-PHBV component.

For D-PHBV8/PHBP11 blend, $X(2230, t)$ shows the same time dependence as $X(1722, t)$, demonstrating that PHBP11 crystallizes simultaneously with D-PHBV8. In addition, the growing rates of $X(\nu, t)$ ($\nu = 1722$ or $2230\ cm^{-1}$) of this blend are rather close to that of D-PHBV8. As a measure of the crystallization rate, the time, $t_{1/2}$, when $X(\nu, t)$ becomes 0.5 was estimated by linear approximation of the data around $X(\nu, t) = 0.5$. The values of $t_{1/2}$ of $X(1722, t)$ for D-PHBV8, PHBP11 and the 1/1 blend are 14, 70 and 20 s, respectively. These results, together with the results of thermal analysis, reveal that PHBP11 crystallizes simultaneously with D-PHBV8 to form cocrystals. The existence of PHBP11 in the blend retards the crystallization of D-PHBV8 probably due to the dilution effect, while D-PHBV8 accelerates the crystallization of PHBP11 by entrapping the latter molecules at the growing front of the crystals. The fact that the crystallization rate of the blend is rather close to that of D-PHBV8 strongly suggest that the crystallization of this blend is leaded by D-PHBV8, i.e. the component crystallizing faster in the pure state. The D-PHBV8 chains, that are about to crystallize at the growing front of a spherulite, may trap the PHBP11 chains in the neighborhood and drag them into the crystalline phase.

For D-PHBV6/PHBP11, on the other hand, $X(2230, t)$ grows faster than $X(1722, t)$. The values of $t_{1/2}$ of $X(1722, t)$ and $X(2230, t)$ for the 1/1 blend are 19 and 15 s, respectively, while those of $X(1722, t)$ for D-PHBV6 and PHBP11 are 11 and 70 s, respectively. Therefore, the crystallization of D-PHBV6 proceeds before the crystallization of PHBP11. During the crystallization of D-PHBV6, PHBP11 molecules get away from the growing front of the spherulite, i.e. the phase segregation precedes the crystallization. The growing rate of $X(1722, t)$ of the blend is, however, yet much higher than the average of pure PHBP11 and D-PHBV6. The preceding crystals of D-PHBV6 probably trap molecules of PHBP11 in the interlamellar regions, which restrict the mobility of PHBP11, and as a result, hasten the crystallization of it. The fact that no sign of two step growth is recognized for $X(1722, t)$ of the blend also supports this indication. Therefore, two crystalline phases must be formed in this blend. Since only one melting peak was observed on the DSC curve of this blend, PHBP11 forms microcrystals of which heat of fusion is too small to be detected by DSC.

4. Discussion

This paper reports on the in situ observation of the crystallization inside a spherulite for the blends of PHBV and PHBP by FTIR microscopy. The crystallization processes of the blend components are traced separately by using deuterated PHBV as a blend component. The C–D and C=O stretching bands in the IR spectra show the behavior of D-PHBV and the whole blend, respectively. In case of the blend of D-PHBV8 and PHBP11 the crystalline peaks of C–D and C=O bands grow simultaneously, indicating the occurrence of cocrystallization. For D-PHBV6/PHBP11, on the other hand, the crystalline peak of C–D band grows faster than that of C=O band, representing the phase segregation preceding the crystallization. These results demonstrate that FTIR microscopy is a powerful tool to trace the formation of different crystalline phases, such as cocrystallization and phase segregation. This method is applicable to various blends, including other blends of bacterial polyesters.

It is rather amazing that the difference in the HV content of only 2% discriminates the crystallization mechanism in D-PHBV/PHBP blends. As possible origin of the difference in the crystallization mechanism between D-PHBV6/PHBP11 and D-PHBV8/PHBP11, we discuss two factors here. One is the difference in the molecular weight of the component copolymers. As well known, fractionation by molecular weight frequently occurs during the crystallization of polymers [29]. In the present case, the difference in molecular weight between D-PHBV and PHBP is certainly large, as shown in Table 1. So, this may be a cause of phase segregation in D-PHBV6/PHBP11 blend. However, the molecular weights of D-PHBV6 and D-PHBV8 are similar, so that the difference in molecular weight cannot be a cause of the difference in the crystallization mechanism between the two blends.

The other factor we should discuss is crystallization rate. The spherulite growth rates of D-PHBV6, D-PHBV8 and PHBP11 decrease in this order as shown in Table 1. The crystallization of the blends are led by the component of faster crystallization, i.e., D-PHBV. The spherulite growth rate of D-PHBV6 is ca. 1.5 times larger than that of D-PHBV8. Therefore, phase segregation must proceed to lower degree before crystallization in D-PHBV6/PHBP11 than in D-PHBV8/PHBP11. D-PHBV6 can drag more PHBP11 chains into crystalline phase than D-PHBV8 does, which must induce the difference in the crystallization mechanism. In order to confirm the effect of crystallization rate on the crystallization mechanism, the analysis of the temperature dependence of $X(1722, t)$ and $X(2230, t)$ for D-PHBV/PHBP and PHBV/D-PHBP blends with various combinations is now in progress and will be reported in a separate paper.

Acknowledgements

This work is partially supported by a Grant-in-Aid for Scientific Research on Priority Area, ‘Sustainable Biodegradable Plastics’, No. 11217205 (2002) from the Ministry of Education, Science, Sports and Culture (Japan).

References

[1] Harris JE, Robeson LM. J Polym Sci B; Polym Phys 1987;25:311.
[2] Alamo RG, Glaser RG, Mandelkern L. J Polym Sci B; Polym Phys 1988;26:2169.
[3] Avella M, Martuscelli E. Polymer 1988;29:1731.
[4] Tanaka H, Lovinger AJ, Davis DD. J Polym Sci B; Polym Phys 1990; 28:2183.
[5] Tashiro K, Stein RS, Hsu SL. Macromolecules 1992;25:180.
[6] Minick J, Moet A, Baer E. Polymer 1995;36:1923.
[7] Morgan RL, Hill MJ, Barham PJ. Polymer 1999;40:337.
[8] Lim SW, Lee KH, Lee CH. Polymer 1999;40:2837.
[9] Pucciariello R, Angioletti C. J Polym Sci B; Polym Phys 1999;37:679.
[10] Qui A, Ikehara T, Nishi T. Polymer 2003;44:3101.
[11] Doi Y, Steinbüchel A, editors. Biopolymers. Polyesters I–III, vol. 3, 3b and 4. Wiley; 2001.
[12] Yoshie N, Menju H, Sato H, Inoue Y. Polym J 1996;28:45.
[13] Yoshie N, Fujiwara M, Ohmori M, Inoue Y. Polymer 2001;42:8557.
[14] Saito M, Inoue Y, Yoshie N. Polymer 2001;42:5573.
[15] Na YH, He Y, Asakawa N, Yoshie N, Inoue Y. Macromolecules 2002; 35:727.
[16] Bluhm TL, Hamer GK, Marchessault RH, Fyfe CA, Veregin RP. Macromolecules 1986;19:2871.
[17] Kamiya N, Sakurai M, Inoue Y, Chûjô R. Macromolecules 1991;24: 2178.
[18] Hiramitsu M, Doi Y. Polymer 1993;34:4782.
[19] Doi Y, Kunioka M, Nakamura Y, Soga K. Macromolecules 1987;20: 2988.
[20] Yoshie N, Menju H, Sato H, Inoue Y. Macromolecules 1995;28: 6516.
[21] Cao A, Kasuya K, Abe H, Doi Y, Inoue Y. Polymer 1998;39: 4801.
[22] Yoshie N, Goto Y, Sakurai M, Inoue Y, Chûjô R, Doi Y. Int J Biol Macromol 1992;14:81.
[23] Gross RA, Ulmer HW, Lenz RW, Tshudy DJ, Uden PC, Brandt H, Fuller RC. Int J Biol Macromol 1992;14:33.
[24] Organ SJ, Barham PJ. Polymer 1993;34:2169.
[25] Yoshie N, Oike Y, Kasuya K, Doi Y, Inoue Y. Biomacromolecules 2002;3:1320.
[26] Kimura T, Ezure H, Tanaka S, Ito E. J Polym Sci Part B; Polym Phys 1998;36:1227.
[27] Matsuda G, Kaji K, Nishida K, Kanaya T, Imai M. Macromolecules 1999;32:8932.
[28] Jiang Y, Gu Q, Li L, Shen DY, Jin XG, Chan CM. Polymer 2003;44: 3509.
[29] Soares JBP, Hamielec AE. Polymer 1995;36:1639.